90

The Engineering Society
For Advancing Mobility
Land Sea Air and Space®
INTERNATIONAL

400 COMMONWEALTH DRIVE, WARRENDALE, PA 15096-0001 U.S.A.

SAE Technical Paper Series

900027

Rapid Compression Machine Measurements of Ignition Delays for Primary Reference Fuels

Pyongwan Park and James C. Keck
Massachusetts Institute of Technology

International Congress and Exposition
Detroit, Michigan
February 26 — March 2, 1990

900027

Rapid Compression Machine Measurements of Ignition Delays for Primary Reference Fuels

Pyongwan Park and James C. Keck

Massachusetts Institute of Technology

ABSTRACT

A rapid compression machine for chemical kinetic studies has been developed. The design objectives of the machine were to obtain: 1) uniform well-defined core gas; 2) laminar flow condition; 3) maximum ratio of cooling to compression time; 4) side wall vortex containment; and, 5) minimum mechanical vibration. A piston crevice volume was incorporated to achieve the side wall vortex containment. Tests with inert gases showed the post-compression pressure matched with the calculated laminar pressure indicating that the machine achieved these design objectives.

Measurements of ignition delays for homogeneous PRF/O_2/N_2/Ar mixture in the rapid compression machine have been made with five primary reference fuels (ON 100, 90, 75, 50, and 0) at an equivalence ratio of 1, a diluent(s)/oxygen ratio of 3.77, and two initial pressures of 500 Torr and 1000 Torr. Post-compression temperatures were varied by blending Ar and N_2 in different ratios. It was found that the ignition delays were not a linear function of the ON of the fuel. Within the experimental range covered, the first-stage ignition delays decreased rapidly as the temperature increased, whereas the second-stage ignition delays stayed unchanged as the temperature increased. Comparison with existing data showed that the ignition delay measurements made in other RCM's should be carefully reevaluated partially due to their high heat transfer characteristics and partially due to their improper mixture preparation procedures.

INTRODUCTION

Spark ignition engine knock is known to be a result of the autoignition of an adiabatically compressed portion of the unburned fuel-air mixture ahead of the advancing flame front [1,2,3]* and obtaining an understanding of this process has been one of the major goals of combustion research [4,5]. In engine studies, primary reference fuels (blends of normal-heptane and iso-octane) are used to establish the octane rating scale, but only limited research on these fuels has been carried out under controlled conditions.

To isolate the autoignition process from the complex engine in-cylinder flow conditions, experimental investigators of knock have used various experimental apparatuses, such as a rapid compression machine, a shock tube, and a combustion bomb [1,6,7,8]. In such devices the autoignition of primary reference fuels has been observed to be either a single- or a two-stage event depending on the physical conditions and the fuel.

An excellent apparatus for observing the two-stage ignition event under engine like conditions is the rapid compression machine (RCM). Unfortunately data obtained in different rapid compression machines operating under similar conditions often disagree [6,7]. The probable reasons for this disagreement are the difficulty of determining the effective temperature of the gas in the presence of turbulent boundary layers and the side wall vortex rolled up by the piston, and the ineffective purging of active species absorbed on the test chamber walls from previous runs.

Since chemistry is very sensitive to the temperature, it is the highest temperature, which occurs in the adiabatic core gas, that controls the reaction rates [1]. It is, therefore, very important to have a well-defined core temperature region in this type of experiment. It is also important to have accurate pressure measurements since these are used to determine the core temperature. In

* Numbers in brackets designate references at end of paper.

some rapid compression machines pressure traces were so masked by mechanical vibrations that obtaining accurate pressure data from these traces was practically impossible [10].

To help solve these problems a new rapid compression machine has been developed in which heat transfer and vibration have been reduced to a minimum and the wall vortex has been captured in a crevice. The performance of the machine was tested with inert gases. Clean pressure traces were recorded with little mechanical vibration. The post-compression pressure agreed with calculated laminar isentropic pressure and the cooling rate of the charge after compression was reduced, indicating that the corner vortex was successfully captured in the crevice.

Autoignition studies for primary reference fuels were also conducted under carefully controlled conditions. The results were quite repeatable with the proper purging procedures described in a following section. It was found that current measured ignition delays agreed with existing data qualitatively, but not quantitatively. The heat transfer characteristics of other rapid compression machines and the purging procedures used were carefully examined. Some of these rapid compression machines were found to have high heat transfer characteristics.

The current measurements of autoignition are believed to be the most accurate since low heat transfer characteristics and little mechanical vibration allowed accurate core temperature determination from the measured pressure trace, and the filling and purging procedures were carefully chosen for repeatability.

EXPERIMENTAL APPARATUS AND PROCEDURE

IDEAL RAPID COMPRESSION MACHINE - The fundamental objective of a rapid compression machine is to heat a test gas as rapidly as possible to high temperature and pressure with as little heat and mass loss as possible. In an ideal machine of this type the temperature T and pressure P of the test gas are related to the compression ratio $CR = V_i/V$ and specific heat ratio $\gamma = C_p/C_v$ by the equations

$$\ln CR = \int_{T_i}^{T} (1/(\gamma'-1))\, d\ln T' \qquad (2.1)$$

and

$$\ln P/P_i = \int_{T_i}^{T} (\gamma'/(\gamma'-1))\, d\ln T' \qquad (2.2)$$

In the derivation of Eq (2.1) and (2.2) it has been assumed that there is no heat or mass loss and the test gas obeys the ideal gas relation of state

$$P\,V = (m_g/W_g)\,R\,T \qquad (2.3)$$

where R is the universal gas constant and V, m_g and W_g are the volume, mass and mean molecular weight of the test gas.

Typical plots of γ as a function of temperature for $i\text{-}C_8H_{18}/O_2/N_2/Ar$ mixtures with various N_2/Ar ratios are shown in Fig. 1 [11,12]. Also shown are corresponding plots of the pressure ratio as a function of the compression ratio and the temperature as a function of the pressure ratio. It can be seen from these plots that to achieve temperature and pressure in the range of 700 to 1000 K and 10 to 100 atm of interest for

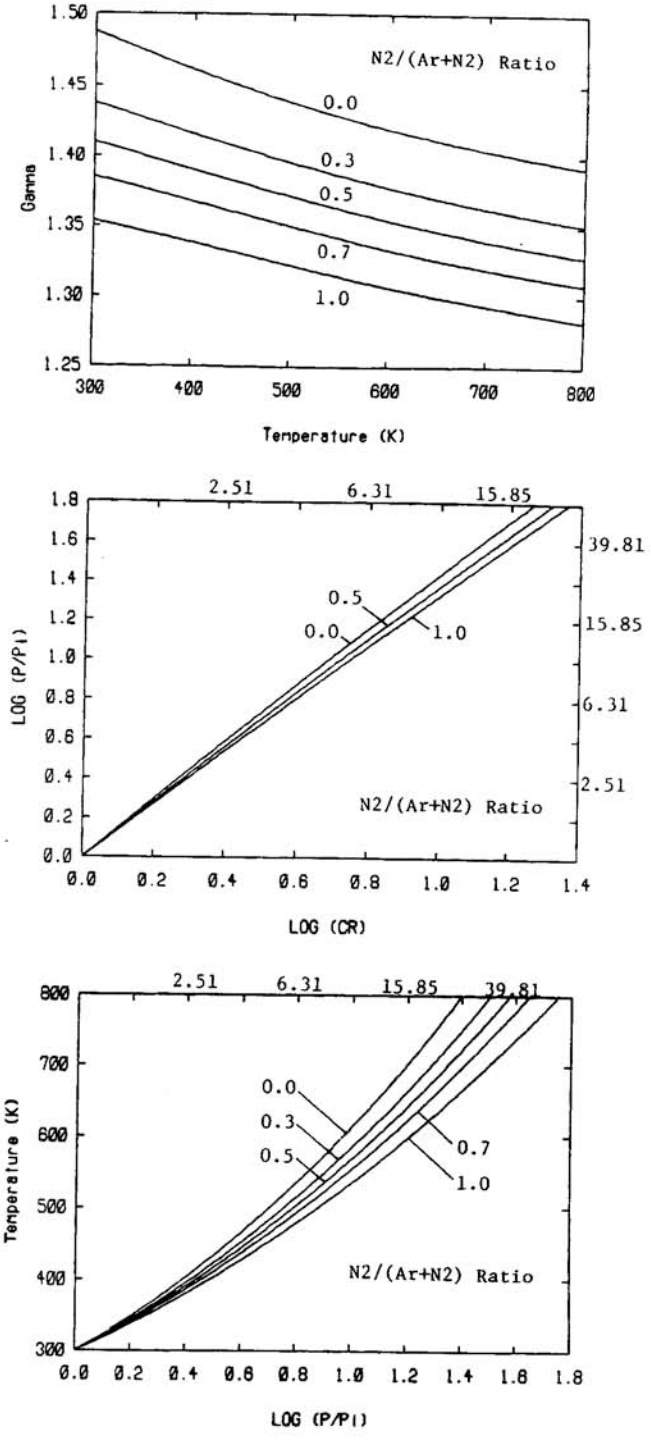

Fig. 1 Specific Heat Ratio, and P,T, and CR Relations for Isentropic Compression of $i\text{-}C_8H_{18}/O_2/N_2/Ar$ Mixture : Equivalence Ratio=1, $(N_2+Ar)/N_2$=3.77, and T_i=300K

the study of autoignition in automobile engines, a compression ratio CR higher than 10 is required for an initial temperature of 300 K and an initial pressure of 1 atm. This is the most basic requirement placed on the design of the present machine.

DESIGN CRITERIA FOR THE CURRENT RCM - In real rapid compression machines, the test time at high temperature is determined by the rate of heat loss from the gas. This will be a minimum if all boundary layers are kept laminar. In a piston-cylinder machine of the type designed and constructed for the present experiment, this requires that the Reynolds number $Re = u_p S/\nu$ based on piston speed u_p, and stroke S, be less than 10^5 i.e.

$$u_p S < \nu\, 10^5 \sim 0.5\ m^2/s \qquad (2.4)$$

where ν is average kinematic viscosity during the compression. Under these conditions the ratio of the laminar boundary layer thickness δ_l to the clearance height h is given by

$$\delta_l / h = (\alpha\, t_q)^{1/2} / h \qquad (2.5)$$

where α is average thermal diffusivity during the compression and t_q is the cooling time. For a well defined adiabatic core, δ_l/h should be less than ~ 0.1 and if a cooling time greater than 100 msec is desired

$$h > 10 \sqrt{\alpha\, t_q} \sim 5\ mm \qquad (2.6)$$

Since the compression ratio is given by the ratio of the stroke S and the clearance height h, the stroke is determined by

$$CR = 1 + S / h \sim 10 \qquad (2.7)$$

$$S = (CR - 1)\, h \sim 5\ cm \qquad (2.8)$$

The maximum piston speed can be determined by combining Eq (2.4) and (2.8) and is given by the relation

$$u_p < \nu\, 10^5 / h\,(CR - 1) \sim 10\ m/s \qquad (2.9)$$

An additional restriction on the piston speed is that it must not be so high that sound waves induced by the piston motion produce any significant variation in temperature. An estimate of these variation can be obtained from the relation

$$\frac{\Delta T}{T} = \frac{1}{2} \frac{u_p^2}{C_p T} = \frac{\gamma - 1}{2} Ma^2 \qquad (2.10)$$

where Ma is the Mach number of the piston. For $\Delta T < 1$ K and $T \sim 1000$ K, the above relation gives $u_p < 20$ m/s which is a somewhat less stringent requirement than Eq (2.9).

A very important phenomenon has not been explicitly taken into account in the design of previous rapid compression machines is the corner vortex caused by the roll-up of the side wall boundary layer during the compression stroke [9]. This places a lower limit on the ratio of the test chamber bore b to the clearance height h. An estimate of the corner vortex diameter d_v can be obtained from the relation

$$\frac{\pi}{4} d_v^2 = u_p \int_0^{t_c} \delta_1\, dt$$

which gives

$$d_v \sim \frac{2}{3} u_p\, (\alpha\, t_c^3)^{1/2} \qquad (2.11)$$

where $t_c = S/u_p$ is the compression time. Combining Eq (2.8) and (2.11), we obtain

$$d_v / h \sim (CR - 1) / Re^{1/4} \qquad (2.12)$$

Since the vortex can be expected to grow with time even after the piston stops, the bore b should be at least 10 times the vortex diameter to insure that an adiabatic core exists during the test time. Combining this condition with Eq (2.12) gives

$$b / h > 10\,(CR - 1) / Re^{1/4} \sim 5 \qquad (2.13)$$

It may be noted that this condition is not met by the Thornton RCM [13] for which b/h ~ 1 and this raises a serious question about the existence of a uniform core gas in this machine.

One technique for dealing with the corner vortex is to introduce a crevice volume at the perimeter of the piston in which it can be contained. The entrance to this crevice must be sufficiently wide to permit the boundary layer to enter and its cross-sectional area must exceed that of the vortex. Although the crevice volume reduces the compression ratio slightly, it prevents the growth of the vortex after compression and reduces heat loss.

In addition to the design restrictions discussed above which are imposed by aerodynamics and thermodynamics, one must also consider the restriction imposed by the requirement that stresses caused by stopping the piston in a very short time do not exceed the yield stress of the materials used to construct the RCM. This imposes a limitation on the maximum deceleration of the piston which is given by

$$a = u_p^2 / 2\, l_s < Y\, A_s / m_p \qquad (2.14)$$

where Y is the yield stress, m_p is the piston mass and l_s and A_s are the piston stopping distance and bearing area. The ratio m_p/A_s can be approximated by $\rho_p L_p$ where ρ_p and L_p are density and length of the piston. This gives

$$l_s > L_p\, (\rho_p\, u_p^2 / 2\, Y) \qquad (2.15)$$

Thus to minimize l_s the piston should be as short as possible and must be constructed of a material with a high yield stress to density ratio. Among the readily available materials, aluminum for which $Y/\rho_p \sim 0.7 \times 10^4\ m^2/s^2$ is an excellent choice.

The relations (2.4) to (2.15) place narrow limits on the design parameters for piston-cylinder RCM's. The values chosen for the present machine are summarized in Table 1. They are remarkably close to those of the M.I.T. machine designed and operated in the 1950's by Taylor et. al. [6]

Table 1. Design Parameters for RCM

test chamber bore	5.08 cm	b
driving chamber diameter	10.16 cm	B
piston length	17.21 cm	L_p
piston mass	0.969 Kg	m_p
stopping pin length	0.10 cm	l_s
corner vortex crevice volume	0.527 cm^3	
clearance height	0.6 - 2 cm	h
maximum stroke	10.92 cm	s
maximum driving pressure	3.45 MPa	P_d
max speed control orfice area	14.19 cm^2	
maximum piston speed	10 m/s	u_p

CURRENT RCM CONFIGURATION - An overall schematic of the machine is shown in Figure 2. The basic design of the piston motion control was adapted from the Thornton rapid compression machine [13], i.e. high pressure gas drive, hydraulic speed control, and pin and groove stopping mechanism. The stationary parts were made from cold-rolled mild steel, whereas the two moving parts, the piston and fast-acting-valve, were made from 6061 aluminum to reduce dynamic stress. Special attention was given to the piston which was made hollow to reduce its mass and to have uniformly distributed stress throughout the body.

To cover a wide range of experimental conditions, the rapid compression machine was designed with easily adjustable stroke, clearance height, piston speed, and initial charge temperature. The stroke can be varied by turning the stroke adjustment screw; the clearance height by changing the clearance height adjustment shim shown in Fig. 3; the piston speed by changing the speed control orfice area and the driving pressure; and the initial charge temperature using an oil bath in the heating jacket. The maximum driving pressure is limited to 3.45 MPa by material stress consideration.

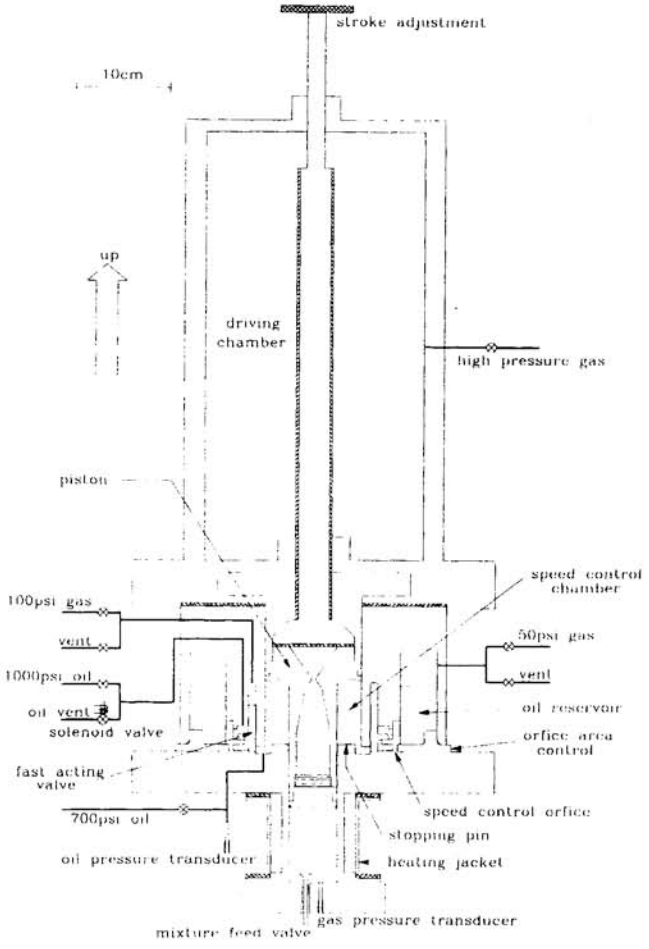

Fig. 2 Sectional View of RCM Assembly

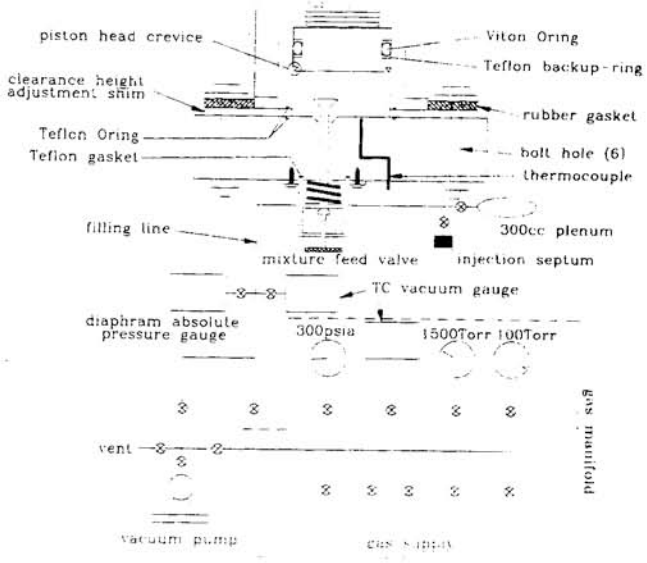

Fig. 3 Test Chamber and Gas Handling System

A detailed drawing of the test chamber and the gas handling system used to prepare fuel, oxygen, and diluent(s) mixtures is shown in Fig. 3. In the test chamber, Teflon O-rings were used for all the static seals, and a Viton O-ring with a Teflon back-up ring was used for the piston dynamic seal. The piston head was machined separate from the piston body so that piston heads with crevice and without crevice could be easily interchanged. As explained earlier, the clearance height could also be changed easily by changing clearance height adjustment shim. To eliminate dead volume, a spring loaded poppet valve was used to seal the test chamber.

Liquid fuel was injected into the machine using a syringe through a rubber septum of the type used in gas chromatographs. A 300 cc plenum was added to the filling line so that gas in the filling line was divided equally between the test chamber and the plenum when new gas was added from the manifold. This helped to reduce the uncertainty in the mixture composition due to back diffusion of gases from the test chamber into the filling line. The measured filling line volume was 45 cm^3 and the gas handling system line volume was 626 cm^3.

INSTRUMENTATION - Static pressures up to 1000 Torr were measured with an MKS 122A diaphram absolute pressure gauge with an accuracy equal to 1% of the reading. Vacuum pressures were measured with thermocouple vacuum gauges.

Dynamic pressures were measured using two Kistler 613 piezoelectric transducers located as shown in Fig. 2. One of these was used to monitor the oil pressure in the speed control chamber and provided information about the piston motion especially the starting and stopping time. The other which was coated with RTV to reduce thermal sensitivity was used to measure the pressure in the test chamber. This pressure transducer is out of plane in Fig. 3. All pressure transducers were calibrated against a dead weight tester and checked at periodic intervals.

The initial charge temperature was measured using a thermocouple located 1 mm below the test chamber as shown in Fig. 3.

All data were recorded and processed using a Transiac 2815 12-bit digitizer controlled by a DSP 4012 controller connected via Camac Crate to a VAX 750 host computer system.

OPERATING PROCEDURE OF THE CURRENT RCM - The basic operating sequence of the machine is as follows:

(1) move the piston and the fast-acting-valve up by pressurizing the oil reservoir with 50 psi gas;
(2) move the fast-acting-valve down by pressurizing the gas chamber above it with 100 psi gas;
(3) lock the fast-acting-valve in position with 1000 psi oil;
(4) lock the piston in position by pressurizing the speed control chamber with 700 psi oil;
(5) pressurize the driving chamber with high pressure gas;
(6) vent the oil reservoir and the gas chamber above the fast-acting-valve;
(7) fire the machine by opening the solenoid valve to relieve the 1000 psi fast-acting-valve locking pressure.

After this sequence, the fast-acting-valve is driven up by the piston locking pressure and the piston is driven down by the driving pressure. Toward the end of the stroke, the piston is slowed down by the stopping pin and groove mechanism [13]. The above sequence does not include mixture preparation which will be explained in detail in section 4 in conjunction with primary reference fuel experiments.

INERT GAS TESTS

Preliminary tests were conducted with inert gases to check the performance of the rapid compression machine and determine the effect of the piston head crevice on heat transfer.

Fig. 4 shows an overlay of two pressure traces from consecutive runs with pure N_2 at the same operating conditions. Time '0' was set to be the inflection point (or the steepest slope point) during the compression stroke since it is well-defined. The machine's performance was quite repeatable since the two pressure traces followed each

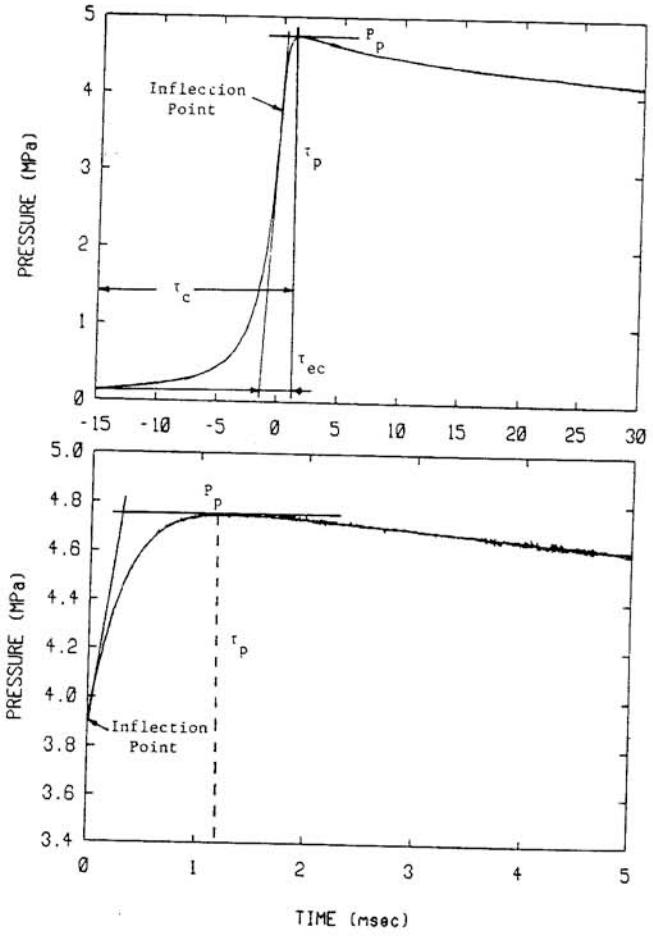

Fig. 4 Typical Pressure Traces for Consecutive Runs with Pure N_2 at Identical Operating Conditions: Piston Head with Crevice, Stroke=9.51cm, Clearance Height=0.615cm, Compression Ratio=15.8, T_i=294K, P_i=1000Torr=0.133MPa, Driving Pressure=2.07MPa, Speed Control Orfice Area=10.58cm^2

other exactly. The compression time, τ_c, is defined to be the time between the piston start and the piston stop, and is measured to be 16 msec from the oil pressure record (the measured oil pressure trace was similar to that for the Thornton machine [13]). The effective compression time, τ_{ec}, is defined as the time between the peak pressure location τ_p and the intersection of the steepest slope line with initial pressure, and is 3 msec. Since the temperature rises most rapidly at the end of compression, the effective compression time should be compared with the ignition delay time, and is of the same order as the shortest total ignition delay time measured.

The upper part of Fig. 5 shows two pressure traces for piston heads with and without the crevice with all other operating conditions kept same. Due to the crevice volume, the peak pressure for the piston head without the crevice is slightly higher than that for the piston head with the crevice, but the pressure drop rate after compression is faster. Isentropic pressures for both cases were calculated using geometric compression ratios, and are shown by lines (1) and (2) in the figure. The corresponding isothermal pressures are shown by line (3) and (4) and the initial pressure by lines (5). It can be seen that the measured pressures are significantly less than the ideal isentropic pressures and that the percentage discrepancy is less for the piston with the crevice. As will be seen below these departure can be attributed to the effects of boundary layers and the corner vortex.

Peak pressures are compared with various calculated pressures on a shorter time scale in the lower part of Fig. 5. Line (6) shows the isentropic pressure for the piston without crevice corrected for the effect of the wall boundary layers using the displacement thickness calculated from the measured pressure traces assuming laminar flow [14]. It can be seen that the calculated pressure is still much higher than the measured peak pressure and the difference is attributed to the effect of the corner vortex. Line (7) shows the pressure calculated for the piston head with the crevice neglecting the boundary layers but assuming that the gas in the crevice is compressed isothermally while that in the test chamber is compressed isentropically. Finally line (8) shows the pressure calculated again assuming isothermal crevice but including the effect of the wall boundary layers in the test chamber. This matches the measured peak pressure almost exactly indicating that for the piston head with the crevice the flow was laminar and the corner vortex was successfully captured in the crevice. The slower pressure drop rate after compression for the piston head with the crevice also indicates that the crevice was successful in reducing heat transfer by suppressing the growth of the corner vortex.

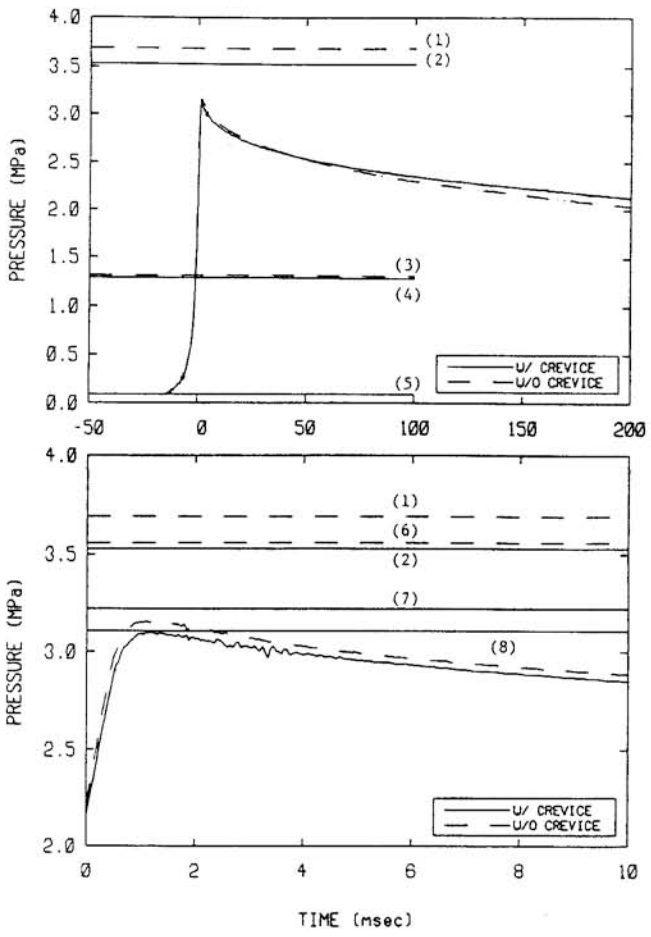

Fig. 5 Comparison of Inert Gas Pressure Traces for Piston Head with and without Crevice : Initial Temperature=298K, Crevice Volume=0.527cm^3, Stroke=7.74cm, Clearance Height=0.60cm, Driving Pressure=2.07MPa, Speed Control Orfice Area=6.81cm^2

GAS : N2	W/O Crevice	W/ Crevice
Isentropic Pressure	(1) 3.69MPa	(2) 3.53MPa
Isothermal Pressure	(3) 1.32MPa	(4) 1.27MPa
Initial Pressure	(5) 95KPa	
Peak Pressure	3.16MPa	3.10MPa
Compression Ratio	13.9	13.4

(6) Isentropic Pressure assuming Laminar Boundary Layer : 3.56MPa, (7) Isentropic Pressure assuming Isothermal Crevice : 3.22MPa, (8) Isentropic Pressure assuming Isothermal Crevice and Laminar Boundary Layer : 3.11MPa

This also agrees qualitatively with Lyford-Pike's experimental observation that a bigger piston head crevice in an engine delays the onset of corner vortex formation during the compression stroke [15].

These inert gas tests provide evidence that the RCM is operating properly and that gas conditions in the test chamber are consistent with expectation based on laminar boundary layers.

PRIMARY REFERENCE FUEL MIXTURE EXPERIMENTS

Throughout the primary reference fuel experiments, the piston head with the crevice was used to reduce heat transfer. The other operating conditions which were kept constant are as follows:

stroke : 9.51 cm
clearance height : 0.615 cm
driving pressure : 2.07 MPa
speed control orfice area : 10.58 cm^2

Before attempting to measure ignition delay times, careful studies were made to ensure reliable and repeatable results. O-rings with the least absorptivity for hydrocarbons were selected and the time to reach saturation was measured. Filling and purging procedures were developed to eliminate carry-over of combustion products from previous runs which were found to affect the measured delay times. Finally a well-defined set of definitions was introduced for the ignition delay times.

O-RING ABSORPTION STUDIES - It is known that many O-ring materials absorb hydrocarbons, therefore Teflon O-rings were used for all seals on the test chamber since it was found that Teflon has the least absorptivity for hydrocarbons. There were places, however, where Teflon O-ring could not be installed due to its stiffness, and Viton O-rings covered with Teflon back-up rings were used in these places.

Fig. 6 shows the test chamber pressures as a function of time after filling with

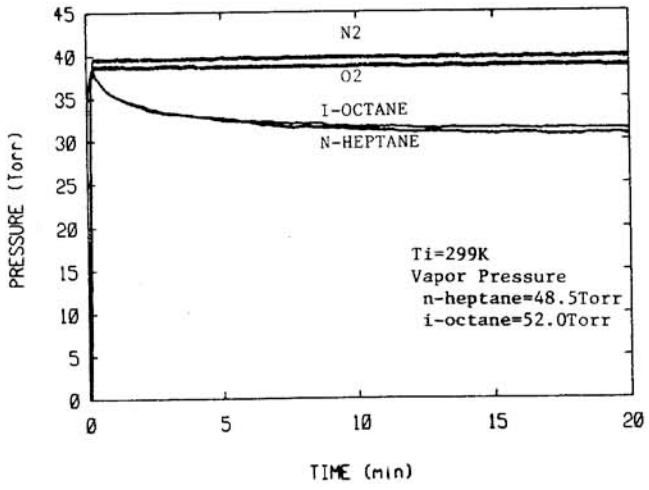

Fig. 6 Pressure in Test Chamber and 300cc Plenum as a Function of Time after Admission of i-C_8H_{18}, n-C_7H_{16}, N_2, and O_2 : Test Chamber Volume=205cc, Plenum+Line Volume=345cc, Amount of Fuel Injected=0.25cc

various gases. For inorganic gases like N_2 and O_2, the pressure remained constant for 20 minutes indicating that there is neither leakage nor absorption. For fuels such as normal-heptane and iso-octane, however, the pressure dropped exponentially with a time constant of approximately 5 minutes to an asymptote where the O-rings are believed to be saturated with hydrocarbons. No significant change in pressure was observed after 10 minutes. Therefore, ten minutes, was determined to be a suitable waiting period for O-ring absorption saturation. As can be seen in Fig. 6, the pressure curves for normal-heptane and iso-octane are almost identical and this is consistent with the fact that the absorption of homologous hydrocarbons such as Alkanes is known to be the same.

It is also important to check that the vapor pressure is high enough at the temperature the fuel is injected to ensure all the liquid is evaporated. For example, at an initial pressure of 1000 Torr, an equivalence ratio of 1, and a diluent(s)/O_2 ratio of 3.77, the partial pressures needed for iso-octane and normal-heptane are 16.8 Torr and 19.0 Torr respectively, and their vapor pressures at 300 K are 54.3 Torr and 50.6 Torr [16].

FILLING AND PURGING PROCEDURES - Initial mixture homogeneity and quiescence in the rapid compression machine must be achieved to insure reliable and repeatable results. Any species left from the previous run should be purged so that an experiment is independent of the previous run.

The following steps were performed for each run:

(1) evacuate the system to a pressure less than 100 millitorr;
(2) inject fuel through the injection septum, and wait for 10 minutes for O-ring absorption saturation;
(3) feed O_2 and diluent(s), and wait another 10 minutes for mixture homogeneity;
(4) fire the rapid compression machine;
(5) reset the rapid compression machine;
(6) evacuate the system;
(7) purge the system with O_2, and evacuate the system;
(8) purge the system with N_2, and evacuate the system;
(9) feed the system with air, wait 10 minutes for any remaining species to diffuse into the air, and evacuate the system;
(10) prepare for the next run, i.e. go to step (2).

The steps (1) to (4) in the above sequence are graphically shown in Fig. 7.

To minimize temperature overshoot and avoid any pre-reactions when various gases were admitted to the test chamber in step (3), they were fed in very slowly by slightly opening the valve connecting the test chamber and the gas manifold. The gas manifold

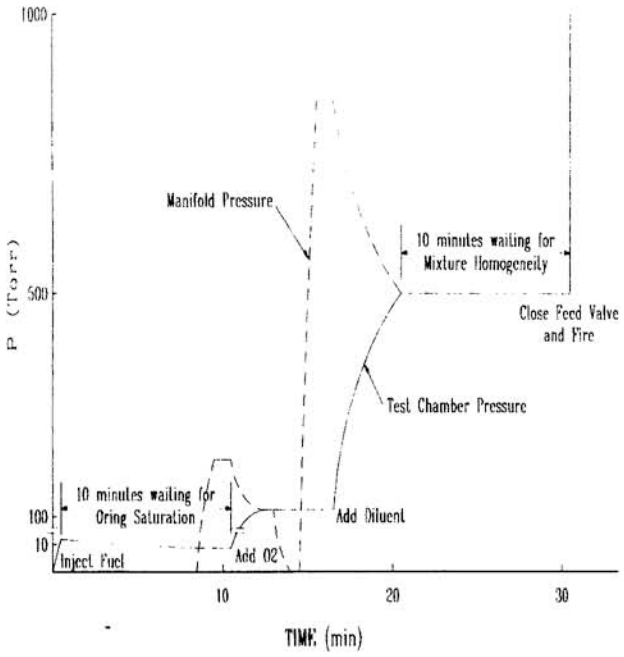

Fig. 7 Primary Reference Mixture Feeding Procedure

pressure, before admitting gas into the test chamber, was set so that the pressure in the test chamber had the desired value when the two pressures equilibrated at the end of the feeding procedure for each gas.

The order of feeding O_2 and diluent(s) was changed to see if the initial mixture homogeneity was achieved, and it was found that the change of feeding order did not have any effect on the experimental results as long as the 10-minute waiting period for the mixture homogeneity was used.

The repeatability of primary reference fuel experiments was checked with the above filling sequence to ensure reliable data since it is known that the repeatability of ignition delay measurements in previous rapid compression machines has been poor. Three consecutive runs at the same operating conditions are shown in the top graph of Fig. 8. It can be seen that the peak pressures are identical but that the ignition delays decreased with increasing run number. This indicates that even though the system was purged three times, there were still species left in the test chamber from the previous run.

To reduce the residual species from the previous run, a new purging procedure was added which involved making a dummy run with pure O_2 before each measurement run. The bottom graph of Fig. 8 shows three consecutive runs made at the same operating conditions after making runs with pure O_2 before each run. The measured ignition delays are no longer ordered and are within 5% of each other. Also the average value is the same as

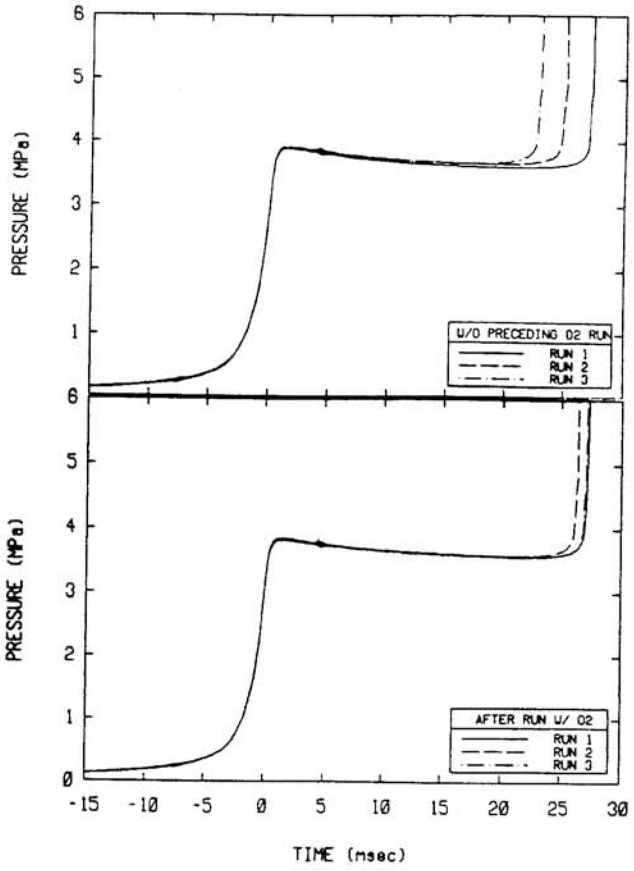

Fig. 8 Effect of Preceding Pure O_2 Run on the Repeatability of Primary Reference Fuel Experiment : Equivalence Ratio=1, N_2/O_2 Ratio=3.77, P_i=1000Torr, T_i=293K, CR=15.8

that for the first run in the top graph. It is believed that the effect of the O_2 run before each primary reference fuel experiment is to burn up active species absorbed on the test chamber walls.

IGNITION DELAY MEASUREMENTS - All the experiments were conducted at an equivalence ratio of 1.0. A mixture of N_2 and Argon was used for the diluents to change the post-compression temperature, and the diluent(s) to O_2 ratio was 3.77. The initial charges were at room temperature (23° ~ 27° C). Five primary reference fuels (ON = 100, 90, 75, 50, and 0) were investigated at two initial pressures (500 Torr and 1000 Torr) and at three N_2/diluent(s) ratios (0.5, 0.7, and 1.0).

Pressure records for different primary reference fuels are superimposed on each other at three different N_2/diluent(s) ratios in Fig. 9 and 10 for two initial pressures of 500 Torr and 1000 Torr respectively. The core temperatures were calculated in two ways, and are given on the right ordinate of the figures. Before there is appreciable heat release by reactions, as in the region marked $\Delta s=0$ in the figure, isentropic relations

based on measured pressure ratios were used to calculate core temperature. Even though a variable specific heat ratio was used for the core temperature calculations, average specific heat ratios are also given in the figures for reader's convenience. When there is appreciable chemical heat release as in the region marked $\Delta v=0$, it is assumed that the boundary layer heat loss is sufficiently small so that a constant volume condition can be used to calculate core temperatures.

The curves in Fig. 9 and 10 show the well known two stage ignition typical of hydrocarbon oxidation in the temperature and pressure range investigated. They can be used to provide a critical test of kinetic models [1,17] of this process and such studies are currently in progress. In this paper only the characteristic ignition delays will be reported.

The definitions of ignition delay times have been unclear and inconsistent in the previous literature. The definitions used in the present study are as follows:

(1) first-stage ignition delay (τ_1): time between the intersection of the steepest slope with the post-compression pressure and the inflection point in the pressure step during first-stage ignition;

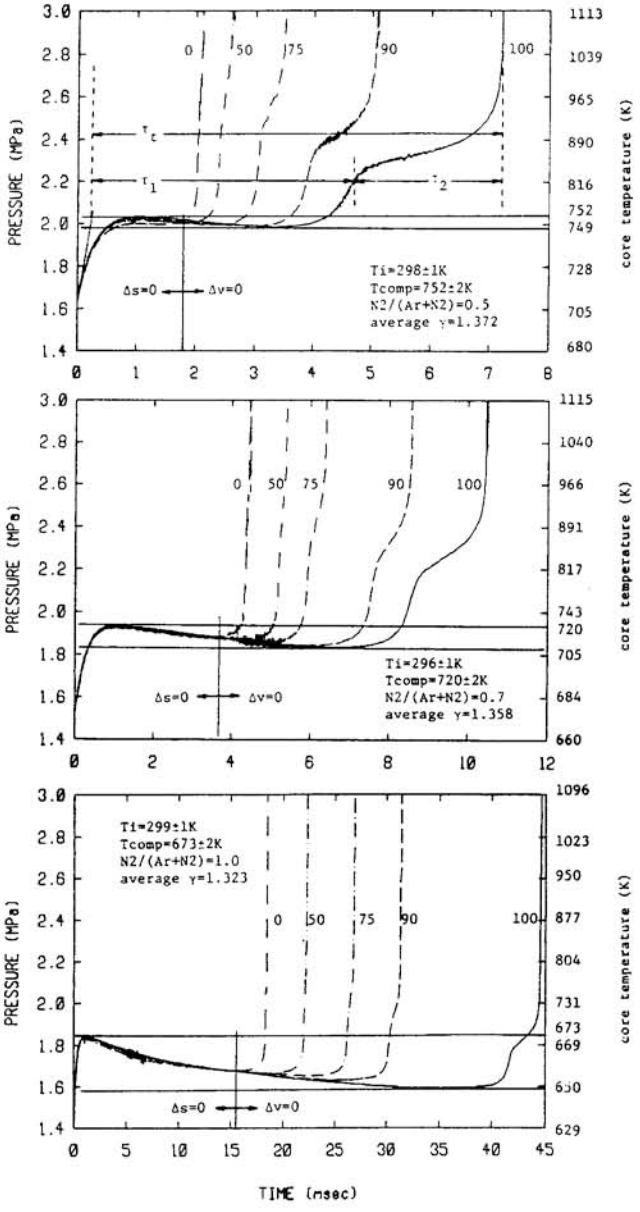

Fig. 9 Pressure Records of Five Primary Reference Fuels at P_i=500Torr : Equivalence Ratio=1, Diluents=N_2+Argon, O_2/Diluents Ratio=3.77, CR=15.8

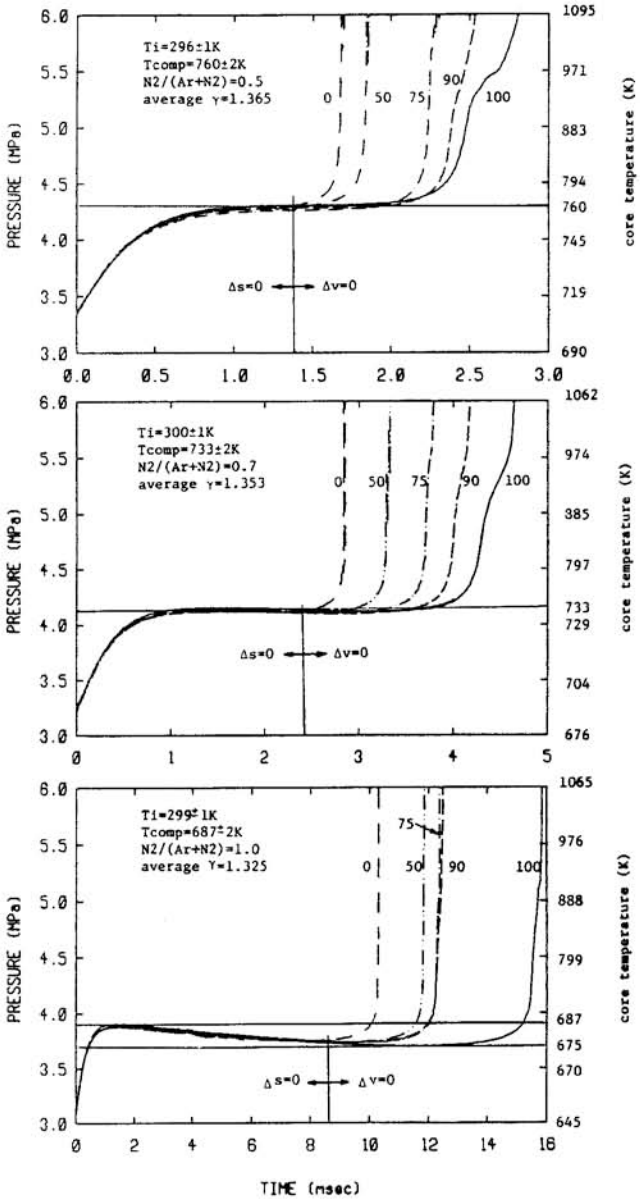

Fig. 10 Pressure Records of Five Primary Reference Fuels at P_i=1000Torr : Equivalence Ratio=1, Diluents=N_2+Argon, O_2/Diluents Ratio=3.77, CR=15.8

(2) second-stage ignition delay (τ_2): time between the inflection point in the pressure step and the point during explosion where core temperature is 1100 K;

(3) total ignition delay (τ_t): sum of τ_1 and τ_2;

The above definitions are shown in the top graph of Fig. 9. The rational for choosing 1100 K as the explosion temperature was that the slope of the pressure was so steep during explosion that there were no differences in ignition delay time measurements when any higher temperatures were used.

The measured total ignition delay times τ_t defined above are shown on an Arrhenius plot in Fig. 11. It is clearly seen that the total ignition delay increases with increasing octane number. It is also seen that ignition delay is not a linear function of octane number and that most of change in ignition delay occurs in the range from octane number 100 to 50. The temperature effect on total ignition delay is monotonic for the experimental range covered and the total ignition delay decreases with increasing temperature. The total ignition delay decreases as the initial pressure increases. These observations are in qualitative agreement with the previous work.

The total ignition delay times normalized by those of iso-octane (ON = 100) are shown as a function of the octane number in Fig. 12. The normalized ignition delay times fall most rapidly between ON = 100 and 50 as observed in

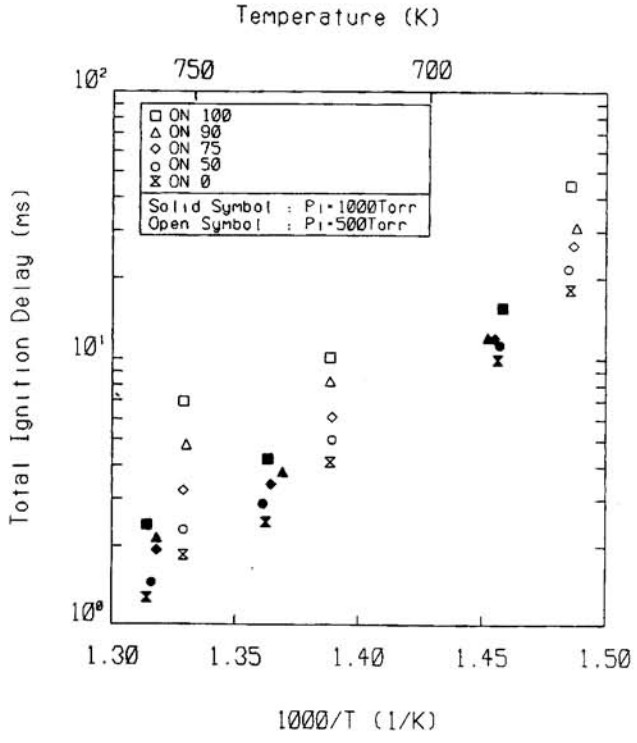

Fig. 11 Measured Total Ignition Delay Times : Equivalence Ratio=1, Diluents=N_2+Argon, O_2/Diluents Ratio=3.77

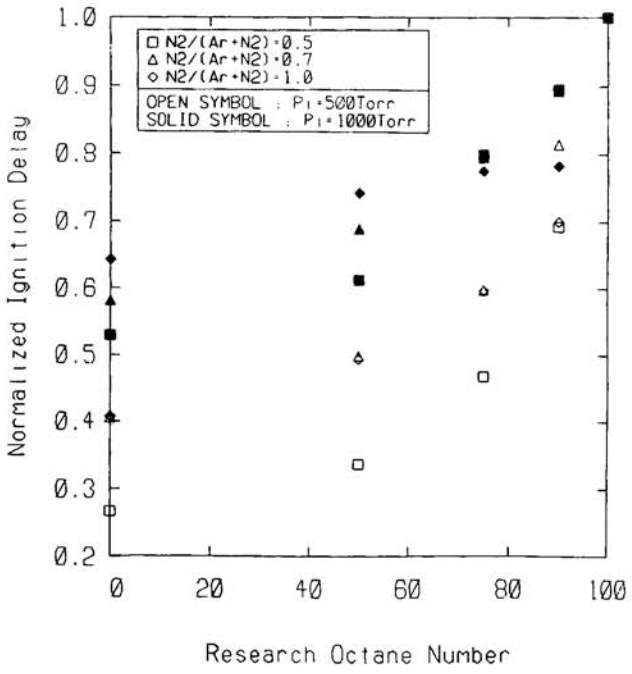

Fig. 12 Normalized Total Ignition Delays : Equivalence Ratio=1, Diluents=N_2+Argon, O_2/Diluents Ratio=3.77

the discussion of Fig. 11. The total spread from ON = 0 to 100 increases as the initial pressure (or density) decreases and decreases as the temperature decreases.

The measured second-stage ignition delay times, τ_2, are shown in Fig. 13. Only values larger than 10^{-1} msec are shown because smaller values could not be measured accurately. It can be seen that the second-stage delay time is a weak function of temperature but increases as the octane number increases and decreases as the initial pressure (density) increases. It can also be seen from a comparison of Figs. 11 and 13 that for the temperature and pressure range investigated, the second-stage delay time is small compared to the total delay time so that most of the delay is due to the first-stage reactions.

COMPARISON WITH EXISTING DATA

Current measured ignition delays were compared with existing data. For iso-octane, data have been reported by Halstead et. al. [7] and Taylor. et. al. [6]. For normal-heptane, the data available were by Taylor et. al. [6] and Rogener's correlation [18].

In their original paper, Halstead et. al. used average temperatures, and they were converted to core temperatures by Hu and Keck [1] using the pressure data provided by original investigators. There were, however, no original pressure data available for Taylor's data, and isentropic temperatures were calculated based on geometric compression

SUMMARY AND CONCLUSION

A rapid compression machine designed for the study of chemical kinetics has been developed. Tests with inert gases show that the flow was laminar and the corner vortex was captured in the piston head crevice. They also strongly suggests the existence of a well-defined adiabatic core gas the temperature of which can be accurately determined from the pressure records. Using this facility, ignition delay measurements have been made with homogeneous fuel/oxygen/diluent(s) mixtures for five different normal-heptane/iso-octane mixtures with octane numbers of 100, 90, 75, 50, and 0 at two initial pressures.

On the basis of the observations, the following conclusions can be drawn for the experimental range covered:

(1) Incorporation of a piston crevice volume helps to suppress the wall vortex and reduce cooling rates;
(2) The repeatability of primary reference fuel experiments was achieved by using a dummy O_2 run between measurement runs, and measured ignition delays were repeatable within 5 percent;
(3) Ignition delays are a nonlinear function of octane number showing little change from 0 to 50 and most change from 50 to 100;
(4) The first-stage ignition delay is a strong function of temperature, but the second-stage ignition delay is a rather weak function of temperature;
(5) At lower initial pressure, the ignition delays are longer and more widely spread with octane numbers;
(6) The current rapid compression machine is a reliable tool for the study of autoignition under well defined conditions;
(7) The present results should be valuable for critical testing of kinetic models of hydrocarbon oxidation.

Further studies at higher temperatures are needed to draw any general conclusions about ignition delay behavior of primary reference fuels in engines.

ACKNOWLEDGEMENT

This work was supported by the U.S. Department of Energy, the Office of Energy Utilization Research, the Energy Conversion and Utilization Technology Program under contract number DE-SG04-87AL44875.

REFERENCES

[1] Hu, H. and Keck, J., "Autoignition of Adiabatically Compressed Combustible Gas Mixture," SAE 872110 (1987).

[2] Taylor, C.F., "The Internal Combustion Engine in Theory and Practice," M.I.T. Press, Cambridge, MA (1984).

[3] Obert, E.F., "Internal Combustion Engines and Air Pollution," Harper & Row Publishers, New York (1973).

[4] Lewis, B. and von Elbe, G., "Combustion, Flames and Explosions of Gases," Academic Press, New York (1987).

[5] Pollard, R.T., "Comprehensive Chemical Kinetics," v.17, C.H. Bamford and C.F.H. Tipper, Eds., Elsevier, Amsterdam (1977).

[6] Taylor, C.F., Taylor, E.S., Livengood, J.C., Russell, W.A., and Leary, W.A., "Ignition of Fuels by Rapid Compression," SAE Quarterly Transaction, v.4, No.2, pp.232 (1950).

[7] Halstead, M.P., Kirsh, L.J., and Quinn, C.P., "The Autoignition of Hydrocarbon Fuels at High Temperatures and Pressures - Fitting of a Mathematical Model," v.30, pp.45 (1977).

[8] Behrens, H., Lehr, H., Struth, W., and Wecken, F., "Shock-Induced Combustion by High Speed Shots in Explosive Gas Mixtures," Dtshc.-Fr. Forschungsinst. Rep. 4/67, Saint-Louis, France (1967).

[9] Tabaczynski, R.J., Hoult, D.P., and Keck, J.C., "High Reynolds Number Flow in a Moving Corner," J. Fluid Mech., v.42, pp.249 (1970).

[10] Halstead, M.P., Kirsh, L.J., Prothero, A., Quinn, C.P., "A Mathematical Model for Hydrocarbon Autoignition at High Pressure," Proc. Roy. Soc., A346, pp.515 (1975).

[11] Reynolds, W.C., "Thermodynamic Properties in SI : Graphs, Tables and Computational Equations for 40 Substances," Dept. of Mech. Eng., Stanford Univ. (1979).

[12] Stull. D.R., Westrum, E.F., and Sinke, G.C., "The Chemical Thermodynamics of Organic Compounds," John Wiley & Sons, Inc., New York (1969).

[13] Affleck, W.S., and Thomas, A., "An Opposed Piston Rapid Compression Machine for Preflame Reaction Studies," Proc. Inst. Mech. Engrs., v.183, No.18, pp.365 (1969).

[14] Keck, J.C. "Thermal Boundary Layer in a Gas Subject to a Time Dependent Pressure," Letters in Heat and Mass Transfer, v. 8, pp. 313 (1981).

[15] Lyford-Pike, E.J., "Measurement and Analysis of Thermal Boundary Layer Thickness in the Cylinder of a Spark Ignition Engine," M.S. Thesis, M.I.T. (1979).

[16] American Petroleum Institute, Project 44 "Selected Values of Physical Properties of Hydrocarbons and Related Compounds," (1953).

[17] Westbrook, C.K., Warnatz, J., and Pitz, W.J., "A Detailed Chemical Kinetic Reaction Mechanism for the Oxidation of Iso-octane and N-heptane over an Extended Temperature Range and Its Application to Analysis of Engine Knock," 22th International Symposium of Combustion, (1988)

[18] von Rogener, H. "Entzundung von Kohlenwasserstoff-Luft-Gemischen durch adiabatische Verdichtung," Z. Elektrochemie, v.53, pp.389 (1949).